2004 International Conference on Image Processing (ICIP)

A NORMALIZED MODEL FOR COLOR-RATIO BASED DEMOSAICKING SCHEMES

Rastislav Lukac and Konstantinos N. Plataniotis

Bell Canada Multimedia Laboratory, The Edward S. Rogers Sr. Department of ECE,
University of Toronto, 10 King's College Road, Toronto, Canada
lukacr@ieee.org, kostas@dsp.utoronto.ca

ABSTRACT

In this paper, a normalized color-ratio model for color filter array (CFA) interpolation schemes is presented. Using the linear scale shift of the input color components the proposed normalized model enforces the underlying modelling assumption in both smooth and high-frequency image regions. Thus, the utilization of the proposed model, which represents a generalization of the conventional colo-ratio model, can significantly boost the performance of most well-known CFA interpolators, in terms of both objective and subjective image quality measures.

1. INTRODUCTION

Single-sensor imaging devices use a single charged couple device (CCD) or a complementary metal oxide semiconductor (CMOS) sensor with a color filter array (CFA) to produce a two-dimensional array or mosaic of color components. Such a CFA image is a low-resolution color image due to fact that only a single spectral component is available at each spatial location. Using the Red-Green-Blue (RGB) Bayer CFA pattern, the restored, high-resolution RGB color image output is obtained by interpolating the missing two color components from the spatially adjacent CFA data [1]. This process is known as CFA interpolation or demosaicking and is an integral part of cost-effective single-sensor devices such as image-enabled wireless phones, pocket-size imaging devices and imaging devices for surveillance and automotive applications.

Demosaicking methods rely on color models to complete the interpolation process. Popular schemes such as the saturation based adaptive interpolation (SAI) scheme [2], the smooth hue transition (SHT) interpolation scheme [3], and the Kimmel's algorithm (KA) [4] employ the color-ratio model introduced in [3]. This model utilizes both the spectral and spatial characteristics of the RGB image and is used to interpolate the missing color components using the neighboring color vectors and the available color component positioned at an interpolation location. Since the model is based on the assumption of uniformity in the smooth areas, it fails interpolating the high-frequency regions. Therefore, an alternative solution is needed.

2. CONVENTIONAL COLOR-RATIO MODEL

Let $\mathbf{x}_{(p,q)} = [x_{(p,q)1}, x_{(p,q)2}, x_{(p,q)3}]$ and $\mathbf{x}_{(i,j)} = [x_{(i,j)1}, x_{(i,j)2}, x_{(i,j)3}]$ be two RGB color vectors with $x_{(p,q)k}$ and $x_{(i,j)k}$, for $k = 1, 2, 3$, denoting the R ($k = 1$), G ($k = 2$) and B ($k = 3$) components. It was argued in [3] that in smooth parts of the image the following hold:

$$x_{(p,q)1}/x_{(i,j)1} = x_{(p,q)2}/x_{(i,j)2} \tag{1}$$

$$x_{(p,q)3}/x_{(i,j)3} = x_{(p,q)2}/x_{(i,j)2} \tag{2}$$

The interpolated value of the R component $x_{(p,q)1}$ is given as $x_{(p,q)1} = x_{(p,q)2}(x_{(i,j)1}/x_{(i,j)2})$ and analogously, the B component is derived via $x_{(p,q)3} = x_{(p,q)2}(x_{(i,j)3}/x_{(i,j)2})$. If the R or B components are used to assist re-interpolating the previously interpolated G component [4], its updated value is obtained via $x_{(p,q)2} = x_{(p,q)1}(x_{(i,j)2}/x_{(i,j)1})$ or $x_{(p,q)2} = x_{(p,q)3}(x_{(i,j)2}/x_{(i,j)3})$.

Since the color-ratio model of (1) and (2) is based on the assumption of uniformity within an image area under consideration, it fails near edge transitions where both the spectral and spatial correlation characteristics of the image vary significantly. As a result, the color-ratio based CFA interpolation schemes produce color artifacts [5].

3. PROPOSED NORMALIZED MODEL

To avoid the problem, a normalized color-ratio model is introduced. The proposed normalization improves the model's characteristics near the edge transitions while preserving the performance in uniform image areas [5]. The normalized color-ratio model utilizes a simple linear shift of the color components. The shift can be controlled by either a non-negative constant or a positive-definite function of the color components inside the localized image area of support.

3.1. Underlying Concept

Let β denote a non-negative shift parameter projecting color components $x_{(p,q)k}$ to $x_{(p,q)k}+\beta$ and $x_{(i,j)k}$ to $x_{(i,j)k}+\beta$, for $k=1,2,3$. Thus, the underlying color-ratio model (1) and (2) changes to [5]:

$$(x_{(p,q)1}+\beta)/(x_{(i,j)1}+\beta)=(x_{(p,q)2}+\beta)/(x_{(i,j)2}+\beta) \quad (3)$$

and

$$(x_{(p,q)3}+\beta)/(x_{(i,j)3}+\beta)=(x_{(p,q)2}+\beta)/(x_{(i,j)2}+\beta) \quad (4)$$

respectively. This suggests that the proposed model generalizes (for $\beta=0$) the conventional color-ratio model of [3]. Simple inspection reveals that in uniform image areas for any arbitrary value of β the normalized ratio $(x_{(p,q)k}+\beta)/(x_{(i,j)k}+\beta)$ is qualitatively identical to the conventional ratio $x_{(p,q)k}/x_{(i,j)k}$. However, near edge transitions the scale shift introduced in the normalized color-ratio model preserves the basic design philosophy of the interpolator while the conventional color-ratio model fails introducing thus shifted colors [5].

Under the new model the unknown R components at an interpolation location is calculated as $x_{(p,q)1}=-\beta+(x_{(p,q)2}+\beta)((x_{(i,j)1}+\beta)/(x_{(i,j)2}+\beta))$. Analogously to this expression, the B component is obtained as $x_{(p,q)3}=-\beta+(x_{(p,q)2}+\beta)((x_{(i,j)3}+\beta)/(x_{(i,j)2}+\beta))$ and the unknown G component can be derived using $x_{(p,q)2}=-\beta+(x_{(p,q)1}+\beta)((x_{(i,j)2}+\beta)/(x_{(i,j)1}+\beta))$ or $x_{(p,q)2}=-\beta+(x_{(p,q)3}+\beta)((x_{(i,j)2}+\beta)/(x_{(i,j)3}+\beta))$.

It will be shown that the interpolator's precision increases with β. For example, in image areas with strong edges or fine details the relationship $x_{(p,q)k}\neq x_{(i,j)k}$ or $x_{(p,q)k}\neq cx_{(i,j)k}$, with a positive constant c identical for each k, is hampering the applicability of the color-ratio model introduced in [3]. On the contrary the linear scale shifting β maps $((x_{(p,q)k}+\beta)/(x_{(i,j)k}+\beta))$ closer to unity, enforcing the underlying modelling assumption for both uniform and detail-rich areas. Since the procedure may shift large, in magnitude, color components beyond the upper limit of the conventionally used 8-bit representation, a reasonable value for the parameter β is $\beta=256$. Such a value constrains the normalized color components during processing within a 9-bit processing range. Straightforward addition of $(-\beta)$ to the intermediate result equivalent to $x_{(p,q)k}+\beta$ maps the interpolated value back into the regular 8-bit range.

3.2. Color Filter Array Interpolator

Application of the normalized color-ratio model to the CFA interpolation schemes is relatively straightforward. The demosaicked procedure interpolates the missing color component $x_{(p,q)k}$ of the three-dimensional RGB color vector $\mathbf{x}_{(p,q)}=[x_{(p,q)1},x_{(p,q)2},x_{(p,q)3}]$ located at the spatial position (p,q) using the available color components of the adjacent vectors $\{\mathbf{x}_{(i,j)}=[x_{(i,j)1},x_{(i,j)2},x_{(i,j)3}];(i,j)\in\zeta\}$, with ζ describing spatial locations of the interpolator inputs. Using the proposed model, an unknown R ($k=1$) or B ($k=3$) component $x_{(p,q)k}$ of the color vector $\mathbf{x}_{(p,q)}$ is interpolated as follows [5]:

$$x_{(p,q)k}=-\beta+(x_{(p,q)2}+\beta)\sum_{(i,j)\in\zeta}\{w'_{(i,j)}\frac{x_{(i,j)k}+\beta}{x_{(i,j)2}+\beta}\} \quad (5)$$

where $w'_{(i,j)}=w_{(i,j)}/\sum_{(i,j)\in\zeta}w_{(i,j)}$ is the normalized edge-sensing coefficient which regulates the contribution of the normalized R/G or B/G ratios $(x_{(i,j)k}+\beta)/(x_{(i,j)2}+\beta)$ to the interpolated output $x_{(p,q)k}$. The normalized G component $(x_{(p,q)2}+\beta)$ and the parameter $(-\beta)$ are used to map the normalized color-ratio interpolator's output to the pixel domain. Assuming a KA-style interpolator which utilizes the G/R and G/B ratios in the re-interpolating of the G components, the interpolator's G output is given as [5]:

$$x_{(p,q)2}=-\beta+(x_{(p,q)k}+\beta)\sum_{(i,j)\in\zeta}\{w'_{(i,j)}\frac{x_{(i,j)2}+\beta}{x_{(i,j)k}+\beta}\} \quad (6)$$

Note that the area of support ζ as well as the weight calculation ($w_{(i,j)}=1$ for non-adaptive schemes) may be appropriately modified depending on the demosaicking scheme employed.

The utilization of the proposed model instead of the conventional color-ratio model in the well-known SHT, SAI and KA schemes, results in their modifications entitled here as the modified SHT (MSHT), the modified SAI (MSAI) and the modified KA (MKA). In order to demonstrate the capability of the proposed model, in addition to the performance of the introduced MSHT, MSAI, and MKA interpolators, a new demosaicking scheme is constructed.

The proposed non-adaptive normalized color-ratio interpolator (NNCRI) produces the restored color image using the four-neighborhood arrangement of the CFA components. The NNCRI scheme interpolates the missing G components $x_{(p,q)2}$ as follows:

$$x_{(p,q)2}=\sum_{(i,j)\in\zeta}\{w'_{(i,j)}x_{(i,j)2}\} \quad (7)$$

where $\zeta=\{(p-1,q),(p,q-1),(p,q+1),(p+1,q)\}$ denotes spatial locations of the available G components forming a diamond-shape mask. The coefficients $w'_{(i,j)}=1/4$ are the normalized weights obtained via the non-adaptive coefficients $w_{(i,j)}=1$ identical for all the neighboring G components $x_{(i,j)2}$, with $(i,j)\in\zeta$.

In the next step, the G components are used interpolating the R and B components. This is done by utilizing the

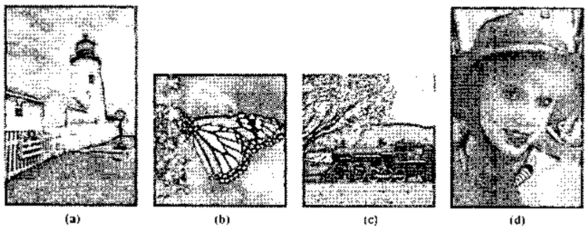

Fig. 1. Test images: (a) Lighthouse, (b) Butterfly, (c) Train, (d) Lady.

normalized color-ratio model of (3) and (4). The resulting interpolator is defined in (5) with $w'_{(i,j)} = 1/4$ and the G component $x_{(p,q)2}$ located at the center of four surrounding R ($k = 1$) or B ($k = 3$) components $x_{(i,j)k}$ forming a square-shape mask $\zeta = \{(p-1, q-1), (p-1, q+1), (p+1, q-1), (p+1, q+1)\}$. An additional interpolation step (5) with $w'_{(i,j)} = 1/4$ and $\zeta = \{(p-1, q), (p, q-1), (p, q+1), (p+1, q)\}$ is need to interpolate the R and B components $x_{(p,q)k}$ located in the original G CFA positions.

After completing the interpolation step, the interpolated G components obtained in (7) are corrected using the proposed interpolator (6) with $w'_{(i,j)} = 1/4$ and $\zeta = \{(p-1, q), (p, q-1), (p, q+1), (p+1, q)\}$. If (p, q) is a position which corresponds to a Bayer pattern R component, then $k = 1$ in (6) is used. Otherwise the position corresponds to a Bayer pattern B component and (6) is defined via $k = 3$. Based on these corrected G components obtained in (6), the interpolation process is completed correcting the R and B components via (5) with $\zeta = \{(p-1, q-1), (p-1, q+1), (p+1, q-1), (p+1, q+1)\}$ and then (5) with $\zeta = \{(p-1, q), (p, q-1), (p, q+1), (p+1, q)\}$. Note that in both aforementioned cases the interpolator is based on the normalized weighted coefficients $w'_{(i,j)} = 1/4$.

4. EXPERIMENTAL RESULTS

Fig.1 depicts the color RGB images (8 bits per channel) used to evaluate the proposed model. Following standard evaluation practices, the original color images are transformed into Bayer CFA images. The restored, full color output are obtained using conventional color-ratio based interpolators (SHT, KA and SAI), and their straightforward modifications (MSHT, MKA, MSAI) which use the normalized color-ratio model with a shift parameter $\beta = 256$. The performance of the NNCRI scheme based on the proposed model is examined as well. Demosaicking performance is measured, objectively, via the mean square error (MSE) and the normalized color difference (NCD) [6].

Fig.2 shows that performance of the methods increases with the parameter β. This confirms that the proposed normalization significantly improves demosaicking performance in high-frequency regions, while preserving the conventional modelling principle in the smooth areas.

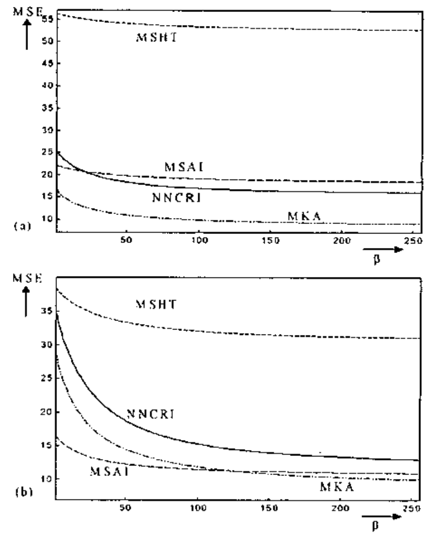

Fig. 2. Performance (MSE) of the proposed normalized color-ratio based interpolators depending on β: (a) the test image Lighthouse, (b) the test image Butterfly.

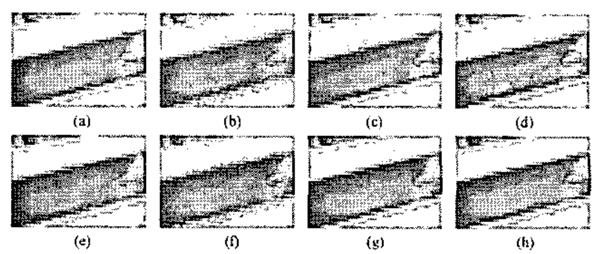

Fig. 3. Enlarged part of the results obtained using the test image Lighthouse: (a) original image, (b) SHT output, (c) SAI output, (d) KA output, (e) NNCRI output, (f) MSHT output, (g) MSAI output, (h) MKA output.

Table 1 and *Table 2* show objective results. As it can be seen the proposed model helps all of the referred demosaicking approaches to improve their performance. In many cases, the utilization of the proposed normalized color-ratio model without the use of the edge-sensing mechanism is more appropriate for reconstruction of fine details and thus, the NNCRI scheme outperforms the edge-sensing interpolators such as the SAI, KA and MSAI schemes.

Enlarged parts of the restored images, shown in *Figs.3-6* are used for subjective (visual) evaluation. The MKA and the NNCRI scheme which use the proposed here normalized color-ratio model produces the best visual quality resulting in naturally colored, sharply restored images with the highest color fidelity compared to the originals.

Table 1. Objective comparison of the performance corresponding to the test images Lighthouse and Butterfly.

Image	Lighthouse		Butterfly	
Method	*MSE*	*NCD*	*MSE*	*NCD*
SHT	58.5	0.0522	41.7	0.0422
SAI	24.3	0.0403	19.0	0.0340
KA	19.4	0.0365	32.2	0.0397
MSHT	53.8	0.0489	33.0	0.0371
MSAI	18.6	0.0329	11.4	0.0257
MKA	9.2	0.0247	10.4	0.0265
NNCRI	16.1	0.0308	13.5	0.0311

Table 2. Objective comparison of the performance corresponding to the test images Train and Lady.

Image	Train		Lady	
Method	*MSE*	*NCD*	*MSE*	*NCD*
SHT	257.7	0.1085	34.7	0.0528
SAI	166.9	0.0866	30.0	0.0485
KA	91.8	0.0710	38.9	0.0530
MSHT	247.0	0.1083	17.7	0.0401
MSAI	156.1	0.0791	12.0	0.0330
MKA	63.7	0.0546	7.8	0.0285
NNCRI	54.8	0.0577	8.5	0.0290

5. CONCLUSIONS

A normalized color-ratio model for CFA interpolation was introduced. The model utilizes linear shifts to alleviate effects of edge variations in the interpolator's input. Employing the proposed model instead of the conventional color-ratio model significantly improves performance of the well-known demosaicking schemes.

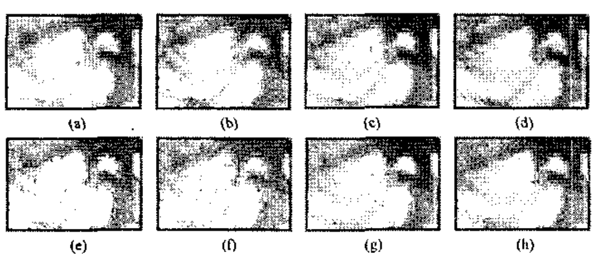

Fig. 4. Enlarged part of the results obtained using the test image Butterfly: (a) original image, (b) SHT output, (c) SAI output, (d) KA output, (e) NNCRI output, (f) MSHT output, (g) MSAI output, (h) MKA output.

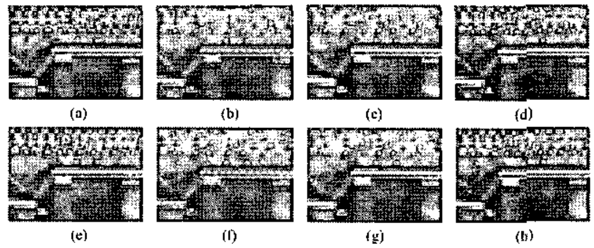

Fig. 5. Enlarged part of the results obtained using the test image Train: (a) original image, (b) SHT output, (c) SAI output, (d) KA output, (e) NNCRI output, (f) MSHT output, (g) MSAI output, (h) MKA output.

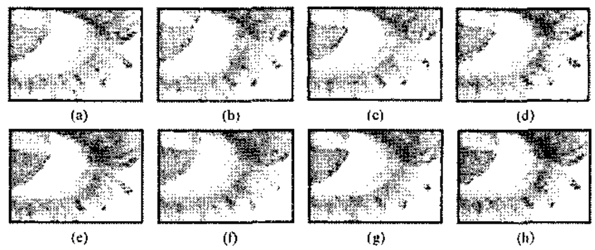

Fig. 6. Enlarged part of the results obtained using the test image Lady: (a) original image, (b) SHT output, (c) SAI output, (d) KA output, (e) NNCRI output, (f) MSHT output, (g) MSAI output, (h) MKA output.

6. REFERENCES

[1] B.E. Bayer, "Color imaging array," U.S. Patent 3 971 065, 1976.

[2] C. Cai, T.H. Yu, and S.K. Mitra, "Saturation-based adaptive inverse gradient interpolation for Bayer pattern images," *IEE Proceedings - Vision, Image, Signal Processing*, vol. 148, pp. 202-208, June 2001.

[3] D.R. Cok, "Signal processing method and apparatus for producing interpolated chrominance values in a sampled color image signal," US Patent 4 642 678, 1987.

[4] R. Kimmel, "Demosaicing: image reconstruction from color CCD samples," *IEEE Transactions on Image Processing*, vol. 8, pp. 1221-1228, September 1999.

[5] R. Lukac and K.N. Plataniotis, "Normalized color-ratio modelling for CFA interpolation," *IEEE Transactions on Consumer Electronics*, vol. 50, May 2004.

[6] K.N. Plataniotis, A.N. Venetsanopoulos, *Color Image Processing and Applications*. Springer Verlag, 2000.